NATIONAL ADVISORY COMMITTEE FOR AERONAUTICS

TECHNICAL NOTE 3361

AERODYNAMIC CHARACTERISTICS OF NACA 0012 AIRFOIL SECTION AT ANGLES OF ATTACK FROM 0° TO 180°

By Chris C. Critzos, Harry H. Heyson,
and Robert W. Boswinkle, Jr.

Langley Aeronautical Laboratory
Langley Field, Va.

Washington
January 1955

NATIONAL ADVISORY COMMITTEE FOR AERONAUTI(

TECHNICAL NOTE 3361

AERODYNAMIC CHARACTERISTICS OF NACA 0012 AIRFOIL SECTION AT ANGLES OF ATTACK FROM 0° TO 180°

By Chris C. Critzos, Harry H. Heyson,
and Robert W. Boswinkle, Jr.

SUMMARY

The aerodynamic characteristics of the NACA 0012 airfoil section have been obtained at angles of attack from 0° to 180°. Data were obtained at a Reynolds number of 1.8×10^6 with the airfoil surfaces smooth and with roughness applied at the leading and trailing edges and at a Reynolds number of 0.5×10^6 with the airfoil surfaces smooth. The tests were conducted in the Langley low-turbulence pressure tunnel at Mach numbers no greater than 0.15.

After the stall with the rounded edge of the airfoil foremost, a second lift-coefficient peak was obtained at an angle of attack of about 45°; initial and second lift-coefficient peaks were also obtained with the sharp edge of the airfoil foremost. The application of roughness and a reduction of the Reynolds number had only small effects on the lift coefficients obtained at angles of attack between 25° and 125°. A discontinuous variation of lift coefficient with angle of attack was obtained near an angle of attack of 180° at the lower test Reynolds number with the airfoil surfaces smooth.

At a Reynolds number of 1.8×10^6, the drag coefficient at an angle of attack of 180° was about twice that for an angle of attack of 0°. The drag coefficients obtained at an angle of attack of 90° at a Reynolds number of 1.8×10^6 were 2.08 and 2.02 with the airfoil surfaces in a smooth and in a rough condition, respectively; the drag coefficient obtained at an angle of attack of 90° and a Reynolds number of 0.5×10^6 with the airfoil surfaces smooth was 1.95. These values compare favorably with the drag coefficient of about 2.0 obtained from the literature for a flat plate of infinite aspect ratio inclined normal to the flow.

INTRODUCTION

A rotary-wing aircraft in forward flight encounters very high local angles of attack at inboard locations of the retreating rotor blades. The local angle of attack may be near 180° where the local rotational

speed is less than the forward speed. In the past, the operation of rotary-wing aircraft has been limited to rather low values of the ratio of forward speed to tip speed so that the area of the very high angle-of-attack region has been small. Consequently, rather crude approximations to the actual airfoil characteristics of the part of the rotor disk operating within this region have been used in rotary-wing analyses with satisfactory results.

Some recent trends toward higher forward speeds for rotary-wing aircraft have resulted in increases in the area of the very high angle-of-attack region, and the forces contributed by this region constitute a greater part of the total rotor forces than in the past. Therefore, airfoil characteristics at very high angles of attack must be available in order to arrive at dependable performance estimates.

Previous investigations have been made of finite-span wings through wide ranges of angle of attack (for example, refs. 1 to 3); however, a search through the literature for similar two-dimensional data yielded only one paper, reference 4, in which the aerodynamic characteristics of the NACA 0015 airfoil section were obtained at angles of attack from 0° to 180°. In order to provide some additional data, a two-dimensional investigation has been made in the Langley low-turbulence pressure tunnel of an NACA 0012 airfoil section for an angle-of-attack range extending through 180°. The NACA 0012 airfoil section was selected because it is a common rotor-blade airfoil section and because its thickness ratio is appropriate, even for high tip-speed rotors, for the inboard part of the blades.

A detailed presentation of the aerodynamic characteristics of the NACA 0012 airfoil section at angles of attack below the stall and for a wide range of Reynolds numbers is contained in reference 5. Thus, only the salient features of the present data obtained in this angle-of-attack range are discussed herein. Some preliminary results of the present investigation have been reported in reference 6.

SYMBOLS

c_d	section drag coefficient
c_l	section lift coefficient
$c_{m_{c/4}}$	section pitching-moment coefficient about quarter-chord point
R	Reynolds number based on airfoil chord
α	section angle of attack

APPARATUS, TESTS, AND METHODS

Wind tunnel.- The present investigation was made in the Langley low-turbulence pressure tunnel. The tunnel, as used in the present tests, had a closed, rectangular test section which was 7.5 feet high and 3 feet wide. Air was used as the test medium.

Model.- The two-dimensional model consisted of the NACA 0012 airfoil section, the coordinates for which are contained in reference 5. The model was machined from solid steel, had a chord of 6 inches, and completely spanned the 3-foot dimension of the tunnel. The maximum deviation of the model coordinates, at the rounded edge of the airfoil, from the specified coordinates is believed to have been 0.003 inch.

Method of mounting models.- The model was supported in the tunnel by a gimbal arrangement at one end and by a multicomponent strain-gage balance at the other end. The gimbals restrained the movement of the model in the lift and drag directions but did not restrain the rotation of the model in the pitch direction. Thus, the balance measured approximately one-half the lift and drag forces and all the pitching moment.

The gimbal arrangement and the balance were located outside the tunnel walls, and each was separated from the model by a labyrinth-type seal mounted flush with the inside surface of the tunnel wall. The seals were approximately 8 inches in diameter and were designed to minimize the effects of leakage through the necessary deflection clearances. Data obtained at conditions of maximum lift and maximum drag over a wide range of pressure differences between the inside and outside of the tunnel indicated that leakage through the seals had no measurable effect on the data presented herein. A more detailed description of a similar model-support arrangement is presented in reference 7.

Tests.- The data in each test were obtained through an angle-of-attack range of about 45°; the limits were established by the rotational range of the end plates to which the model was attached. Angles of attack from 0° to 360° were obtained by attaching the model to the end plates at various rotational locations. Measurements of lift, drag, and pitching moment were made at angles of attack of 4°, or less, apart.

Tests were made with the model surfaces smooth and with roughness applied on the leading and trailing edges of the model. For the tests with the model surfaces smooth, the surfaces were polished to a high degree of smoothness when the model was installed in the tunnel. The surfaces were also wiped clean at the beginning of each test. For the tests with roughness, 0.005-inch-diameter carborundum grains were spread over a surface length equal to 8 percent of the chord measured from the leading and trailing edges on both the upper and lower surfaces. The grains were spread to cover from 5 to 10 percent of this area.

With the model surfaces smooth, data were obtained through an angle-of-attack range from 0° to 360° at a Reynolds number of approximately 1.8×10^6 and from 0° to 180° at a Reynolds number of approximately 0.5×10^6. With roughness applied on the model, data were obtained through an angle-of-attack range from 0° to 180° at a Reynolds number of approximately 1.8×10^6. The stagnation pressure and the Mach number were 1 atmosphere and 0.15, respectively, in the tests at the lower Reynolds number and 4 atmospheres and 0.12, respectively, in the tests at the higher Reynolds number.

Corrections.- Theoretically derived expressions were used to correct the lift, drag, and pitching-moment data for the effects of the solid blockage caused by the constriction of the flow past the model and for the distortion of the lift distribution caused by the induced curvature of the flow. Corrections to account for the effects of the blockage caused by the wake were obtained from measurements of the pressures on the walls at a point directly above and at a point directly below the model. Details of these corrections are discussed in reference 8.

Precision of measurements.- The force and moment beams used in the multicomponent strain-gage balance employed in the present investigation were designed to give measurement accuracies within 0.1 percent of their design maximum loads. On this basis, the accuracies of the force and moment coefficients are shown in the following table:

	$R = 0.5 \times 10^6$	$R = 1.8 \times 10^6$
c_l	±0.049	±0.017
c_d	±0.016	±0.006
$c_{m_{c/4}}$	±0.017	±0.006

On the basis of repeatability of the data, however, the accuracies are believed to be considerably better than indicated in this table.

RESULTS AND DISCUSSION

Results at $R = 1.8 \times 10^6$ with airfoil surfaces smooth.- The aerodynamic characteristics of the NACA 0012 airfoil section, as obtained in the present investigation at a Reynolds number of 1.8×10^6 with the airfoil surfaces smooth, are presented in figure 1 for angles of attack from 0° to 360°.

A maximum section lift coefficient, having a value of 1.33 (fig. 1), occurs at an angle of attack of about 14°. A second lift-coefficient peak, having a value of 1.15, is shown at an angle of attack of about 45°. The second lift-coefficient peak is much less abrupt than the initial one.

As would be expected for a symmetrical airfoil section, initial and second lift-coefficient peaks, having values negative to those obtained at 14° and 45°, are obtained at 346° and 315°, respectively. For the sharp edge foremost, initial and second lift-coefficient peaks having magnitudes of 0.77 and 1.07, respectively, also occur.

The minimum value of the section drag coefficient, although not shown clearly in figure 1, was found to be about 0.007 with the rounded edge foremost; however, with the sharp edge foremost, a minimum value of about 0.014 was obtained. Beyond the stall, the section drag coefficient increased with angle of attack until a maximum value of 2.08 was reached at angles of attack of 90° and 270°.

The section pitching-moment coefficient is shown in figure 1 to become negative after the stall ($\alpha \approx 14°$) and to remain negative to $\alpha = 180°$. The variation of pitching-moment coefficient with angle of attack is antisymmetrical about an angle of attack of 180°.

The variations of the force and moment coefficients with angle of attack immediately beyond the stall are shown in figure 1 to be functions of the direction of change of angle of attack; the direction in which the angle of attack was changed in this region is indicated in figure 1 by arrows. As the angle of attack was increased beyond the stall, the lift coefficient is higher and the drag coefficient is lower than the values obtained with the angle of attack decreasing from some higher angle.

Cross plots of figure 1 yielded the drag polar of figure 2(a) and the pitching-moment polar of figure 2(b). It may be noted in figure 2(a) that the lift coefficient has a positive finite value at an angle of attack of 90° and a negative finite value at 270°. The finite values of the lift coefficient at these angles of attack can probably be attributed to the fact that some lift is being realized over the rounded edge of the airfoil. The finite value of the pitching-moment coefficient at zero angle of attack in figure 2(b) is probably the result of a slight asymmetry in the model.

Effects of applying roughness and of reducing the Reynolds number.- The application of roughness at the leading and trailing edges of the airfoil at a Reynolds number of 1.8×10^6 is shown in figure 3(a) to have only small effects on the lift coefficients obtained at angles of attack from 25° to 125°. However, at the stall with the rounded edge of the airfoil foremost, the effect of roughness was to reduce the maximum lift coefficient from 1.33 to 1.07. Roughness is also shown to reduce the initial and second lift-coefficient peaks obtained with the sharp edge foremost and to reduce slightly the lift-curve slope near $\alpha = 180°$.

At angles of attack from 0° to 165°, reducing the Reynolds number from 1.8×10^6 to 0.5×10^6 with the airfoil surfaces smooth is shown to

have effects on the lift coefficient similar to those obtained by the application of roughness. However, at a Reynolds number of 0.5×10^6, the initial lift-coefficient peak obtained with the sharp edge foremost was slightly higher than that obtained at a Reynolds number of 1.8×10^6. Also, at the lower Reynolds number, the variation of the lift coefficient with angle of attack near an angle of attack of 180° is quite different from that obtained at the higher Reynolds number. Details of this variation are discussed in the subsequent section.

The application of roughness at a Reynolds number of 1.8×10^6 is shown (fig. 3(a)) to reduce the drag coefficient at $\alpha = 90°$ from a value of 2.08 to 2.02; reducing the Reynolds number from 1.8×10^6 to 0.5×10^6 with the airfoil surfaces smooth results in a reduction of the drag coefficient at $\alpha = 90°$ to a value of 1.95. Thus, the surface condition and the Reynolds number are shown to have a noticeable effect on the drag at an angle of attack of 90°. It might be expected that the lower drag coefficients obtained at $\alpha = 90°$, with roughness or with the lower Reynolds number, might be the result of delayed or incomplete separation at the rounded edge. If this were the case, the lower drag coefficients should be accompanied by higher lift coefficients than were obtained for the higher Reynolds number condition with the airfoil surfaces smooth. However, the validity of this expectation cannot be corroborated by the present results since the differences in the lift coefficients for the three test conditions at an angle of attack of 90° are small and within the experimental accuracy.

Application of roughness and reduction of the Reynolds number are shown in figure 3(a) to have only small effects on the pitching-moment coefficients.

The effects (shown in fig. 3(a)) of reducing the Reynolds number and of the application of surface roughness on the force and moment coefficients for an angle-of-attack range from -2° to 32° are presented in greater detail in figure 3(b); these effects are typical of what has been obtained with many airfoil sections in the past and therefore are not discussed further.

Details of lift curves near $\alpha = 180°$.- The lift curves obtained near $\alpha = 180°$ with the model surfaces smooth (fig. 3(a)) are presented in greater detail in figure 4. At a Reynolds number of 1.8×10^6 (fig. 4(a)), the lift coefficient is shown to be a continuous function of angle of attack through an angle of attack of 180°. The small discontinuity in lift coefficient at $\alpha = 182°$ is probably due to small angle-of-attack errors in alining the model previous to one or both of the tests in which data were obtained at this nominal angle of attack.

At a Reynolds number of 0.5×10^6 (fig. 4(b)), it may be noted that not only does the lift coefficient appear to be a discontinuous function

of angle of attack, but also the discontinuity occurs at an angle slightly greater than 180° for the increasing angle of attack and at an angle slightly less than 180° for the decreasing angle of attack. It may also be noted that some differences are evident in the data obtained from two tests in which the angle of attack was increased from different angles of attack below 180° to angles of attack beyond 180°. The data of figure 4(b) indicate that the hysteresis effect persists all the way to the stall. Comparison of the data of figure 4(b) with those of figure 4(a) indicates that larger values of lift are obtained at the lower Reynolds number all the way from the discontinuity to the stall.

The phenomena just described were thought to have the following explanation: With the airfoil producing positive lift near an angle of attack of 180°, the flow over the sharp airfoil edge produces a small separated flow region on the upper surface, after which the flow reattaches to the surface; the boundary layer is turbulent from the point of reattachment to the downstream separation point. On the lower surface the favorable pressure gradient, which exists on the surface for a great distance from the upstream edge of the airfoil, is conducive to a laminar boundary layer from the upstream edge of the airfoil to the separation point. In the region of the high adverse pressure gradient at the rounded, downstream edge of the airfoil, the laminar boundary layer on the lower surface would be expected to separate at a more upstream location than the turbulent boundary layer on the upper surface. Under such circumstances, the flow in the vicinity of the downstream edge of the airfoil would be somewhat similar to that over an airfoil having a small positive flap deflection. The sudden change (fig. 4(b)) from an effective positive flap deflection to an effective negative flap deflection would occur, of course, when the boundary layer on the lower surface became turbulent and the boundary layer on the upper surface became laminar. The hysteresis shown in figure 4(b) probably results from the rather complicated relationship between the pressure field around the airfoil and the region of separated flow. Separation points are dependent upon the distribution of surface pressure; however, the pressure distribution in turn depends not only upon the boundary shape of the airfoil but also upon the extent and location of the regions of separation.

On the basis of the preceding explanation, the presence of turbulent boundary layers on both the upper and lower surfaces of the airfoil should eliminate the discontinuity in the lift curve. The absence of the discontinuity at a Reynolds number of 1.8×10^6 (fig. 4(a)) suggests that transition has occurred on the surface upstream of the point at which laminar separation took place at the lower Reynolds number (fig. 4(b)).

In an effort to obtain some additional information on these phenomena, lift data near $\alpha = 180°$ were obtained at a Reynolds number of 0.5×10^6 with roughness on the leading and trailing edges of the airfoil. The purpose of applying the roughness was to establish turbulent boundary layers on both airfoil surfaces which, again, would be expected to

eliminate the discontinuity in the lift curve. The results obtained were rather inconclusive, however, in that some of the effective-flap effects were still evident in the data. The roughness in this experiment was the same as that used in the previously discussed tests at the higher Reynolds number, and the possibility exists that this size of roughness at the lower Reynolds number was insufficient to cause complete transition to a turbulent boundary layer on both surfaces.

Comparison of present results with those obtained in other facilities.- The present results obtained with the NACA 0012 airfoil section in the Langley low-turbulence pressure tunnel (Langley LTPT) are compared in figure 5 with hitherto unpublished data obtained with the NACA 0012 airfoil section in the Langley 300 MPH 7- by 10-foot tunnel (Langley 7 × 10) and with data from reference 4 obtained with the NACA 0015 airfoil section.

The data of the present investigation, shown in figure 5, were obtained at a Reynolds number of 1.8×10^6 with the airfoil surfaces smooth. Curves are shown for the data as obtained (uncorrected for tunnel-wall effects), corrected for tunnel-wall effects by the method of reference 8 (same data as in fig. 1), and corrected for tunnel-wall effects by the equations of reference 9. Application of the tunnel-wall corrections of either reference 8 or 9 to the present lift and drag data is shown in figure 5 to yield essentially the same result even for the drag coefficient at an angle of attack of 90°.

The investigation in the Langley 300 MPH 7- by 10-foot tunnel was made at a Reynolds number of 1.36×10^6 and a Mach number of about 0.20. The 1-foot-chord model used in these tests completely spanned the 7-foot dimension of the tunnel so that the ratio of airfoil chord to tunnel height was 1.5 times the ratio for the present investigation. The Langley 300 MPH 7- by 10-foot tunnel data were corrected by the equations of reference 9 and the corrected data, as shown in figure 5, are in good agreement with the corrected data of the present investigation.

The tests of reference 4 were made at a Reynolds number of 1.23×10^6 with a 1.5-foot-chord NACA 0015 airfoil section spanning the shorter dimension of a 2.5- by 9-foot tunnel. The indicated airspeed of the tests is stated in reference 4 to have been 80 miles per hour; the lift and drag characteristics were determined from both force and pressure measurements. Only the results of the force measurement are presented in figure 5. A conclusion, based on some experiments and assumptions, was reached in reference 4 that tunnel-wall corrections to the data presented therein were unnecessary.

The lift and drag coefficients for the NACA 0015 airfoil section as obtained in reference 4 are shown in figures 5(a) and 5(b) to be much less than those for the NACA 0012 airfoil discussed previously. The differences in the data obtained with the two sections appear greater than could be attributed to a change in thickness ratio from 12 to 15 percent. Use of the pressure measurements from reference 4 for the comparisons

would yield no better overall agreement in the lift variations and would yield poorer agreement in the drag variations since the friction drag would not be included. Application of tunnel-wall corrections (for example, those of ref. 9) would result in even greater disparity in the data obtained with the two sections.

The drag coefficient for a flat plate of infinite aspect ratio inclined normal to the flow is found in the literature (for example, refs. 10 to 13) to be very nearly 2.0. This value compares favorably with the drag coefficients obtained in the present investigation with the airfoil at an angle of attack of 90°.

The data of reference 10 show a marked effect of aspect ratio on the drag of a flat plate at $\alpha = 90^\circ$. For example, the drag coefficient of a flat plate having an aspect ratio of 20 is shown to be about 1.48 in comparison with the two-dimensional value of 2.0. As pointed out in reference 6, this result emphasizes a basic question, not yet resolved, as to how two-dimensional data should be applied to a rotating wing for those cases in which the flow over one surface is characterized by extensive regions of separation.

CONCLUSIONS

The following conclusions may be made regarding the results of an investigation of the aerodynamic characteristics of the NACA 0012 airfoil section at angles of attack from 0° to 180°:

1. After the stall with the rounded edge of the airfoil foremost, a second lift-coefficient peak was obtained at an angle of attack of about 45°. Initial and second lift-coefficient peaks were also obtained with the sharp edge of the airfoil foremost. The values of the lift coefficient at the initial and second peaks with the rounded edge of the airfoil foremost and at the initial and second peaks with the sharp edge foremost were 1.33, 1.15, 0.77, and 1.07, respectively, at a Reynolds number of 1.8×10^6 with the airfoil surfaces smooth.

2. A small finite value of the lift coefficient obtained at an angle of attack of 90° was probably the result of realizing some lift over the rounded edge of the airfoil.

3. Application of surface roughness at the leading and trailing edges and reduction of the Reynolds number had only small effects on the lift coefficients obtained at angles of attack between 25° and 125°.

4. At a Reynolds number of 0.5×10^6 with the airfoil surfaces smooth, a discontinuous variation of lift coefficient with angle of attack was obtained near an angle of attack of 180°; this result is

believed to have been caused by a difference in the chordwise locations of the separation points on the upper and lower surfaces.

5. At a Reynolds number of 1.8×10^6 with the airfoil surfaces smooth, the section drag coefficient at an angle of attack of 180° was about twice that at an angle of attack of 0°.

6. The drag coefficients obtained at an angle of attack of 90° and a Reynolds number of 1.8×10^6 were 2.08 and 2.02 with the airfoil surfaces smooth and rough, respectively; the drag coefficient obtained at an angle of attack of 90° at a Reynolds number of 0.5×10^6 with the airfoil surfaces smooth was 1.95. These values compare favorably with the drag coefficient of about 2.0 obtained from the literature for a flat plate of infinite aspect ratio inclined normal to the flow.

7. The quarter-chord pitching-moment coefficient became negative after the stall and remained negative until an angle of attack of 180° was reached.

8. The data of the present investigation were found to be in good agreement with results obtained with a different model of the same airfoil section in another facility where the ratio of airfoil chord to tunnel height was 1.5 times larger than that for the present investigation.

Langley Aeronautical Laboratory,
National Advisory Committee for Aeronautics,
Langley Field, Va., October 11, 1954.

REFERENCES

1. Knight, Montgomery, and Wenzinger, Carl J.: Wind Tunnel Tests on a Series of Wing Models Through a Large Angle of Attack Range. Part I - Force Tests. NACA Rep. 317, 1929.

2. Lock, C. N. H., and Townend, H. C. H.: Lift and Drag of Two Aerofoils Measured Over 360° Range of Incidence. R. & M. No. 958, British A.R.C., 1925.

3. Shirmanow, P. M.: I. - Yawing Moment of an Isolated Air-Foil. II. - Test of an Air-Foil at Angles of Incidence From 0° to 360°. Rep. No. 271, Trans. CAHI No. 36 (Moscow), 1928.

4. Pope, Alan: The Forces and Pressures Over an NACA 0015 Airfoil Through 180 Degrees Angle of Attack. Georgia Tech. Rep. No. E-102, Daniel Guggenheim School of Aeronautics, Feb. 1947. (Summary of paper also available in Aero Digest, vol. 58, no. 4, Apr. 1949, pp. 76, 78, and 100.)

5. Loftin, Laurence K., Jr., and Smith, Hamilton A.: Aerodynamic Characteristics of 15 NACA Airfoil Sections at Seven Reynolds Numbers From 0.7×10^6 to 9.0×10^6. NACA TN 1945, 1949.

6. Loftin, Laurence K., Jr.: Airfoil Section Characteristics at High Angles of Attack. NACA TN 3241, 1954.

7. Loftin, Laurence K., Jr., and Von Doenhoff, Albert E.: Exploratory Investigation at High and Low Subsonic Mach Numbers of Two Experimental 6-Percent-Thick Airfoil Sections Designed To Have High Maximum Lift Coefficients. NACA RM L51F06, 1951.

8. Abbott, Ira H., Von Doenhoff, Albert E., and Stivers, Louis S., Jr.: Summary of Airfoil Data. NACA Rep. 824, 1945. (Supersedes NACA WR L-560.)

9. Allen, H. Julian, and Vincenti, Walter G.: Wall Interference in a Two-Dimensional-Flow Wind Tunnel, With Consideration of the Effect of Compressibility. NACA Rep. 782, 1944. (Supersedes NACA WR A-63.)

10. Wieselsberger, C.: Airplane Body (Non Lifting System) Drag and Influence on Lifting System. Vol. IV of Aerodynamic Theory, div. K, ch. II, sec. 1, W. F. Durand, ed., Julius Springer (Berlin), 1935, pp. 141-146.

11. Wieselsberger, C.: Versuche über den Luftwiderstand gerundeter und kantiger Körper. Ergebn. Aerodyn. Versuchsanst. Göttingen, Lfg. II, 1923, pp. 33-34.

12. Prandtl, Ludwig: Essentials of Fluid Dynamics. Hafner Pub. Co. (New York), 1952, p. 182.

13. Fluid Motion Panel of the Aeronautical Research Committee and Others: Modern Developments in Fluid Dynamics. Vol. I, ch. I, sec. 10, S. Goldstein, ed., The Clarendon Press (Oxford), 1938, p. 37.

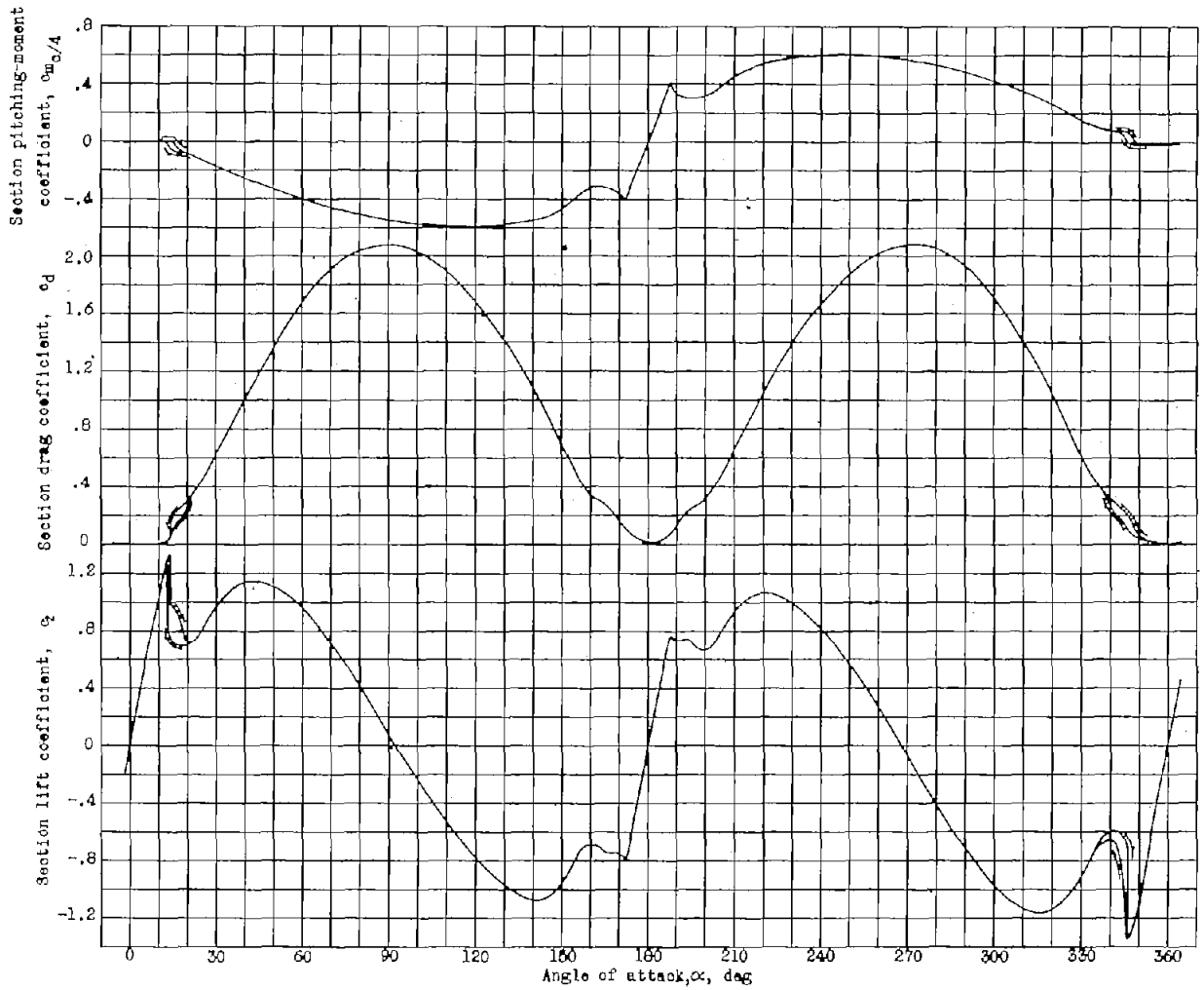

Figure 1.- Aerodynamic characteristics of NACA 0012 airfoil section. $R = 1.8 \times 10^6$; airfoil surfaces smooth. Symbols for data points are shown in figure 5.

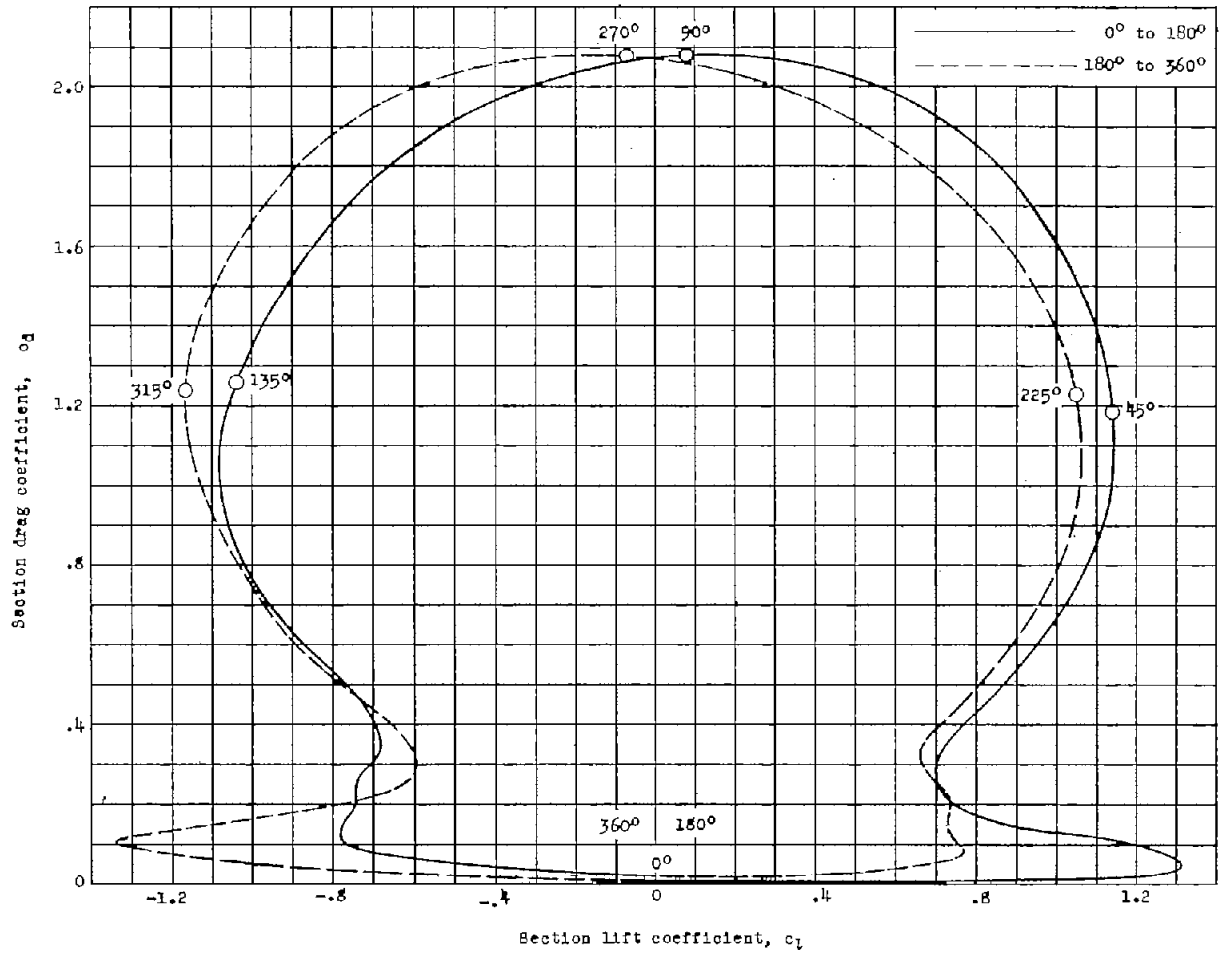

(a) Drag.

Figure 2.- Variations of section drag and pitching-moment coefficients with section lift coefficient for NACA 0012 airfoil section. $R = 1.8 \times 10^6$; airfoil surfaces smooth.

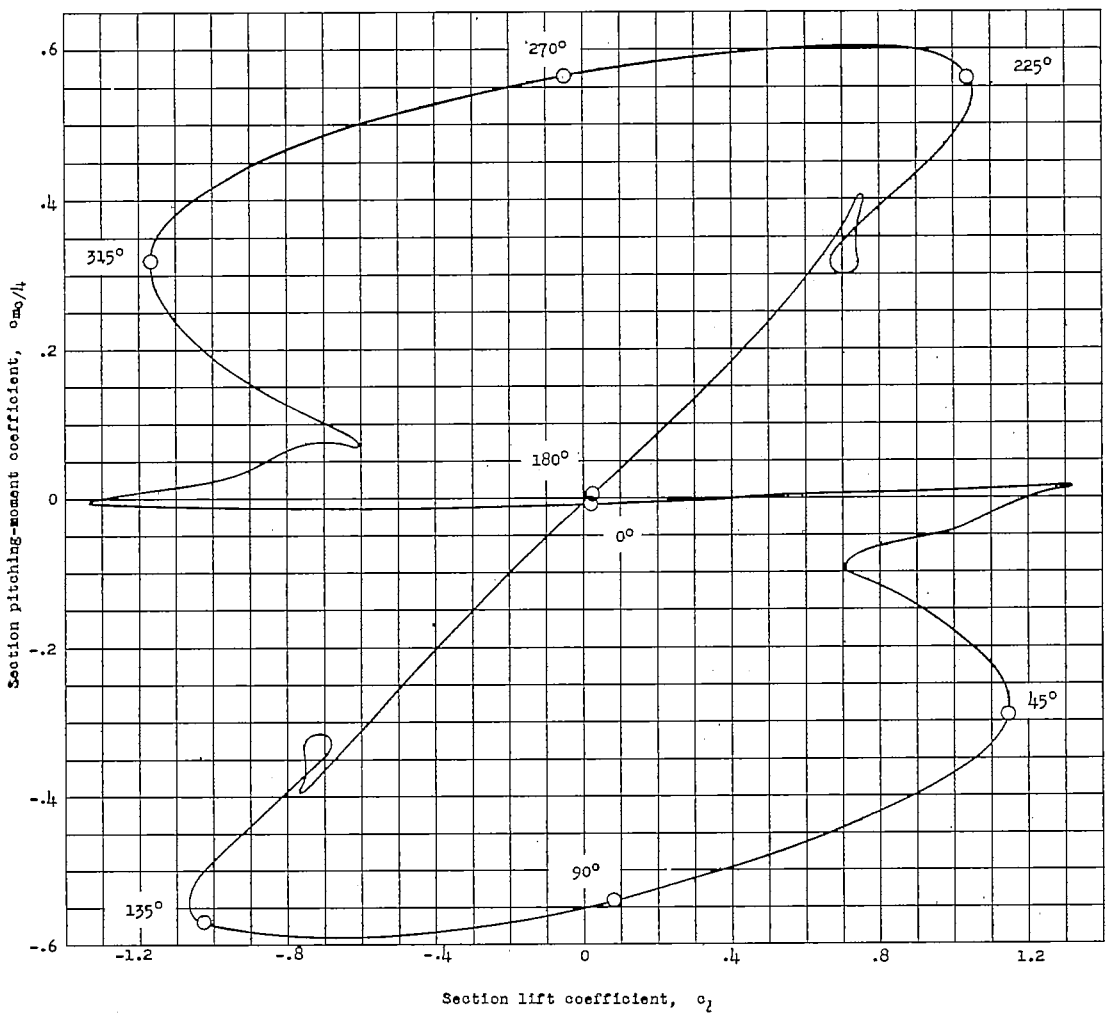

(b) Pitching moment.

Figure 2.- Concluded.

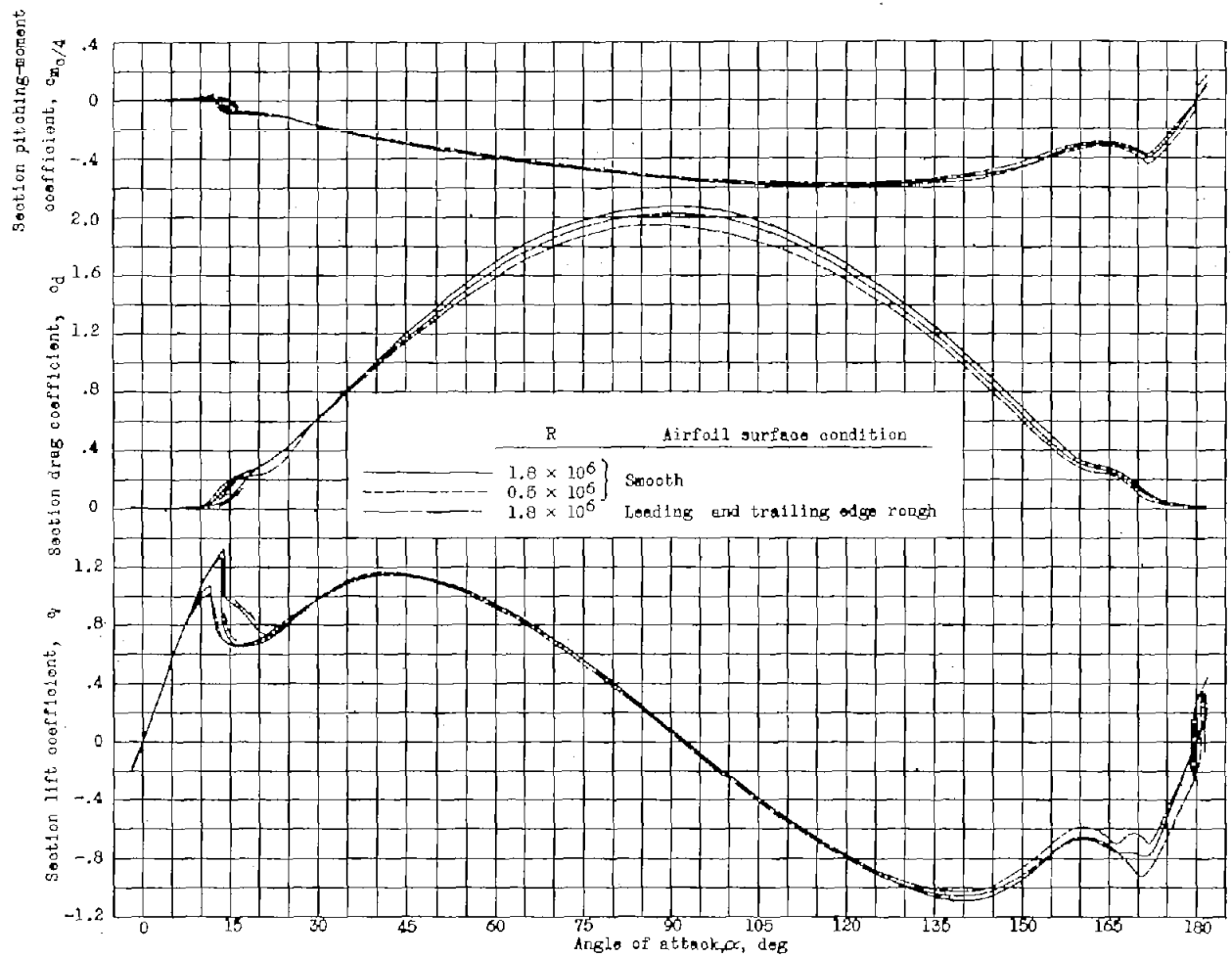

(a) Angles of attack from -2° to 182°.

Figure 3.- Effect of Reynolds number and surface conditions on aerodynamic characteristics of NACA 0012 airfoil section.

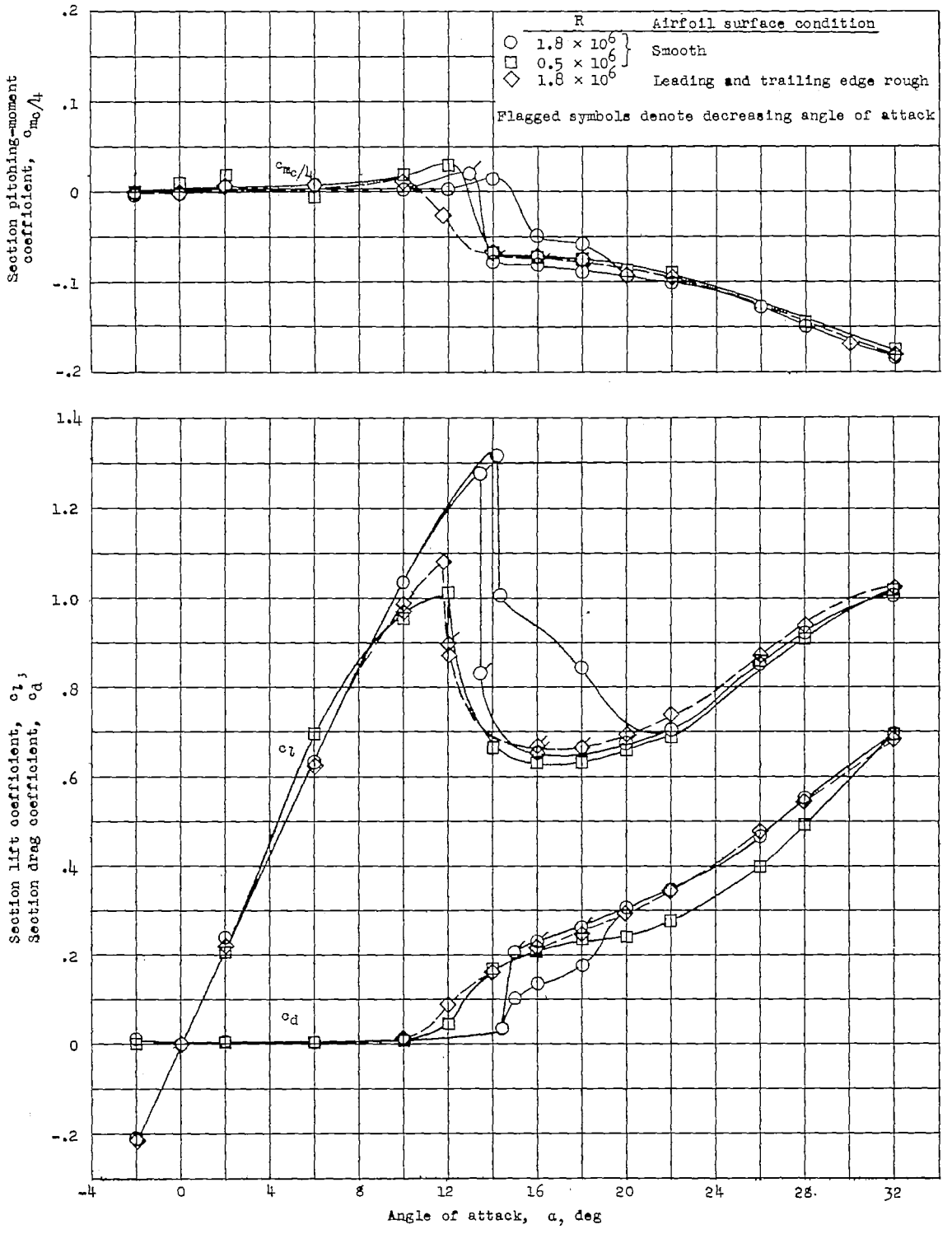

(b) Angles of attack from -2° to 32°.

Figure 3.- Concluded.

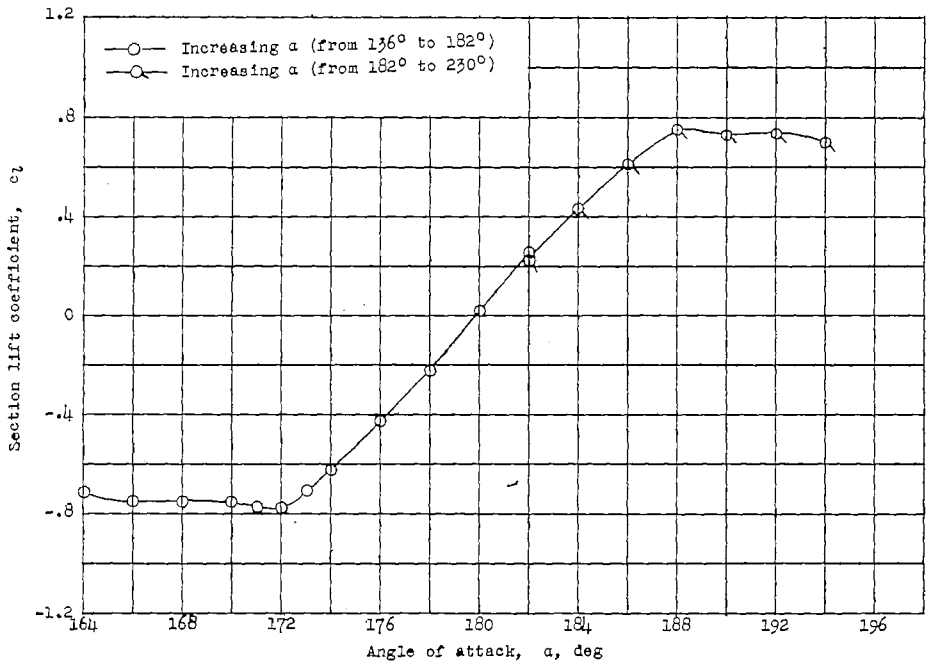

(a) $R = 1.8 \times 10^6$.

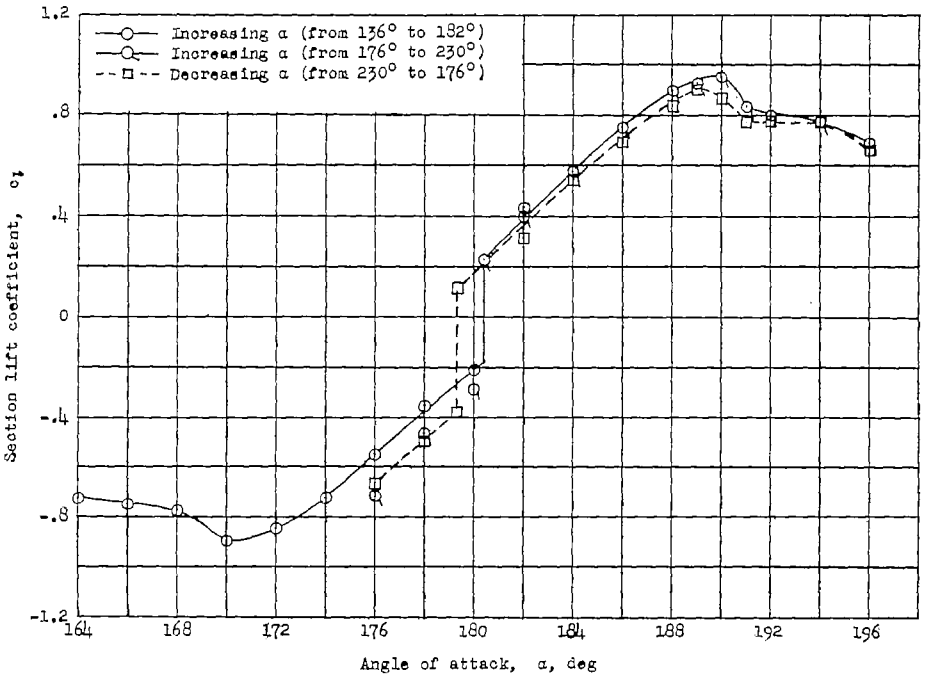

(b) $R = 0.5 \times 10^6$.

Figure 4.- Variation of section lift coefficient with angle of attack for NACA 0012 airfoil section in smooth condition near an angle of attack of 180°.

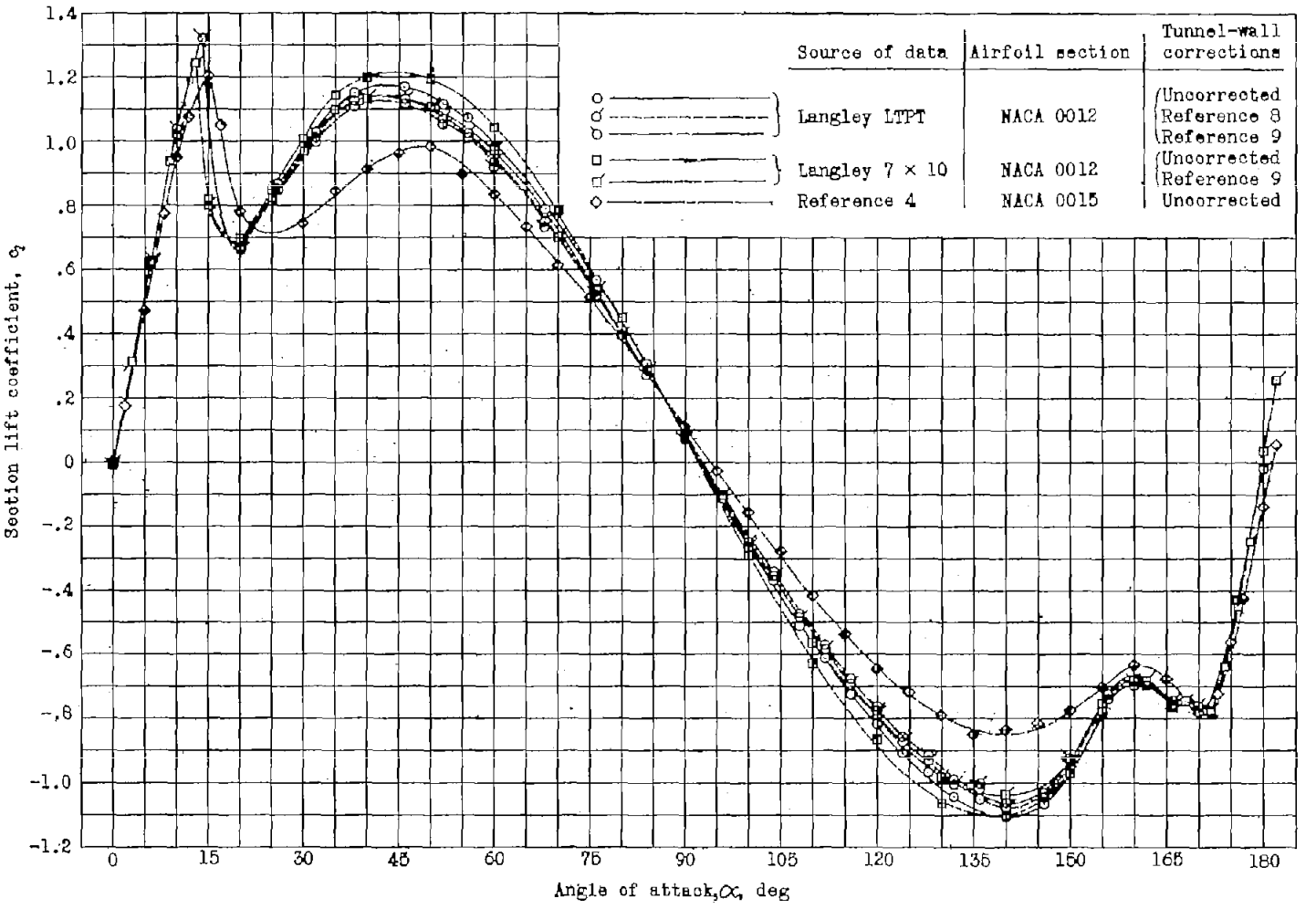

(a) Lift.

Figure 5.- Comparison of present results with those obtained in other facilities.

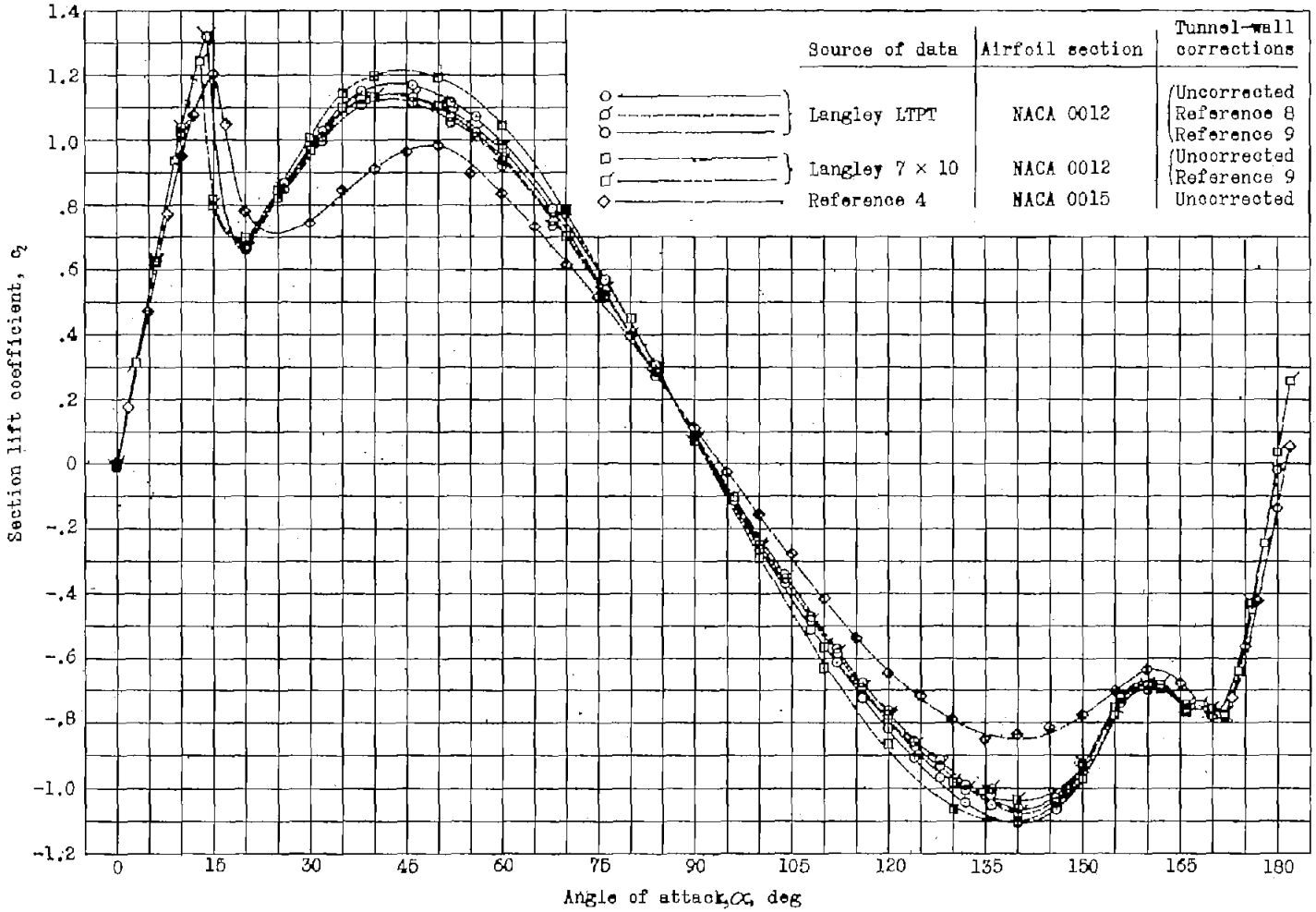

(a) Lift.

Figure 5.- Comparison of present results with those obtained in other facilities.

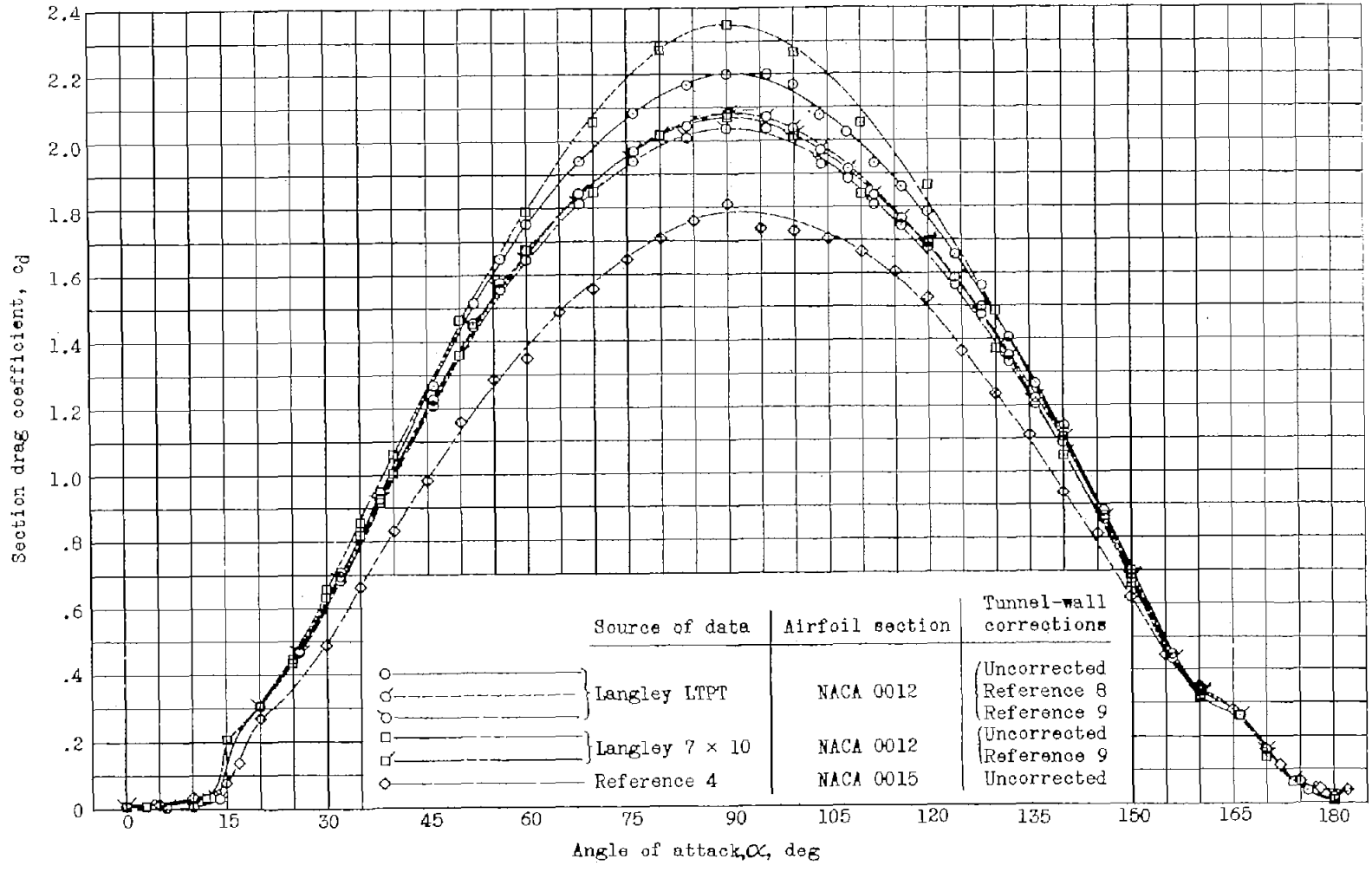

(b) Drag.

Figure 5.- Continued.

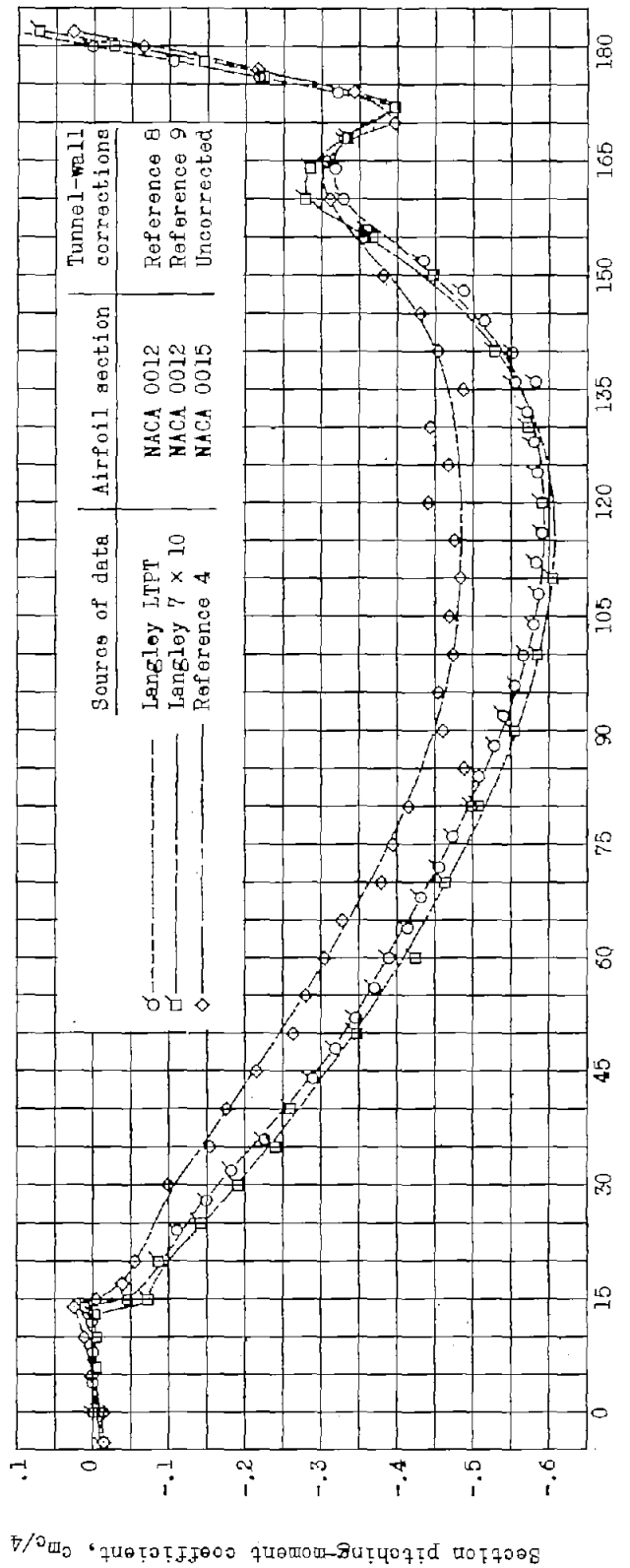

(c) Pitching moment.

Figure 5.- Concluded.